Sorption and interfacial rheology study of model asphaltene compounds.

Diego Pradilla*,[1], Sébastien Simon[1], Johan Sjöblom[1]

[1]Ugelstad Laboratory, Department of Chemical Engineering, Norwegian University of Science and Technology (NTNU), NO-7491 Trondheim, Norway.

Joseph Samaniuk [2], Marta Skrzypiec [3], Jan Vermant [2]

[2] Soft Materials Laboratory, Department of Materials, ETH Zürich, Vladimir-Prelog-Weg 5, 8093 Zürich, Switzerland

[3]Institute of Chemical Technology and Engineering, Poznan University of Technology, Berdychowo 4, 60-965 Poznan, Poland

*Corresponding Author

E-mail: diego.c.p.ragua@ntnu.no
Phone: +47 735 94 080

Notes

The authors declare no competing financial interest.

KEYWORDS: Dilatational rheology, shear rheology, desorption, asphaltene model compounds.

Abstract

The sorption and rheological properties of an acidic polyaromatic compound (C5PeC11), which can be used to further our understanding in the behavior of asphaltenes, are determined experimentally. The results show that C5PeC11 exhibits the type of pH-dependent surface activity and interfacial shear rheology observed in C_6-asphaltenes with a decrease in the interfacial tension concomitant to the elastic modulus when the pH increases. Surface pressure-area (Π-A) isotherms show evidence of aggregation behavior and π-π stacking at both the air/water and oil/water interfaces. Similarly, interactions between adsorbed C5PeC11 compounds are evidenced through desorption experiments at the oil/water interface. Contrary to indigenous asphaltenes, adsorption is reversible, but desorption is slower than for non-interacting species. The reversibility enables us to create layers reproducibly, whereas the presence of interactions between the compounds enables us to mimic the key aspects of interfacial activity in asphaltenes. Shear and dilatational rheology show that C5PeC11 forms a predominantly elastic film both at the liquid/air and the liquid/liquid interface. Furthermore, a soft glassy rheology model (SGR) fits the data obtained at the liquid/liquid interface. Yet, it is shown that the effective noise temperature determined from the SGR model for C5PeC11 is higher than for indigenous asphaltenes measured under similar conditions. Finally, from a colloidal and rheological standpoint, the results highlight the importance of adequately addressing the distinction between the material functions and true elasticity extracted from a shear measurement and the apparent elasticity measured in dilatational-pendant drop set-ups.

1. Introduction

Asphaltenes are commonly defined as the fraction of petroleum insoluble in *n*-alkanes (such as heptane or hexane) but soluble in aromatic compounds (such as toluene or xylene)[1]. These surface active polar compounds are largely responsible for problems during production, transport and refining of crude oil resulting in higher production costs[2]. For example, asphaltenes can precipitate and deposit in the reservoirs, wells, pipes and other equipment[3, 4, 5]. They can also stabilize water-in-oil emulsions[6] (W/O) by forming a solid-like interface , or "skin" [7, 8] , at the oil/water interface that hinders coalescence and retards film drainage[9, 10, 11]. This "skin" is due to interfacial asphaltene-crowding[12] enhanced by self-association at the liquid-liquid interface and even the build-up of multilayers[13]. The properties of this interfacial film need to be understood and characterized and interfacial rheology is an adequate tool to fulfill such goal.

Shear, dilatational, and mix-field flow types can be obtained in interfacial rheological techniques. In simple shear experiments, flow is induced at a constant area, while in dilation the area of the interface is changed. Studies on interfacial shear rheology[14, 15] using a biconical geometry showed that asphaltenes form films of high elasticity after several hours of aging. Furthermore, a concentration threshold range of 2-5 g/L was found for the formation of the mechanically strong film at the oil/water interface after aging. Samaniuk et al.[12] recently studied asphaltenes at the hexadecane/water interface using a double wall-ring (DWR) geometry confirming the effects of concentration and aging. They also concluded that: (i) asphaltene films at the oil/water interface behave as soft-glassy materials, (ii) the crowding of the interface plays a crucial role and, (iii) the concentration/frequency-dependent data is in agreement with a soft-glassy rheology (SGR) model. Using a similar geometry, Harbottle et al.[16] showed that the microstructure of the asphaltene network film at the oil/water interface can be liquid-like or solid-like depending on the initial bulk concentration, aging time of the interface and solvent aromaticity. The transition states could be related to the yield stress which might act as an energy barrier against drop coalescence.

The literature regarding interfacial dilatational rheological studies of asphaltene films at the liquid-liquid interface is extensive[17, 18, 19, 20, 21, 22]. It is imperative to emphasize that in such experiments, depending on the dominating phenomena, the nature of the measured quantities will vary. For instance, at interfaces largely dominated by interfacial tension, the influence of the exchange with the bulk is dominant (adsorption/desorption dynamics), whereas extra mechanical stresses are essentially negligible; this is often the case for low molecular weight surfactants. At interfaces dominated by extra stresses, as in the case of particle monolayers or asphaltenes that clearly exhibit a skin, the nature of the elastic response is fundamentally different. Hence, when discussing the moduli extracted from dilatational experiments it should be noted that these may not always be true material functions.

Literature studies report a behavior that is somewhat general to asphaltenes. First, the apparent elastic dilatational modulus (E') increases with time and concentration. This is an indication of the kinetic build-up of the film, crowding and possible cross-linking of asphaltenes at the interface. Second, a maximum in E' with concentration is observed, the location will depend on the conditions of the experiment and asphaltene origin[18, 20, 21, 22]. And third, if the aged interface is contracted, a phenomenon described as crumpling was observed[20].

The exchange of surfactant between the bulk and the interface and its effects on the apparent elastic dilatational modulus are typically described using the Lucassen van den Tempel (LvdT) approach[23] which assumes that the adsorption at the interface is diffusion-controlled and reversible. The application of the LvdT model to asphaltenes has, however, been less successful. Two explanations have been so far put forward: first, asphaltenes adsorb irreversibly to oil/water interfaces and give rise to an extra mechanical stress at the interface[12]. Second, the diffusion coefficient tends to be low and to vary with concentration[18].

From the broad definition of asphaltenes as a solubility class, and therefore polydisperse, it follows that they are heterogeneous in chemical composition. The different functionalities, molecular weights, and molecular architectures make it challenging to obtain a complete understanding of their properties. Sjöblom et al[24]. indicated two main strategies that can be used to tackle this issue: fractionation of the complete asphaltene content into sub-fractions of reduced complexity (but still polydisperse[25, 26] and different among reservoirs[27]) or synthesis of model molecules of defined chemical structure that mimic aspects of the chemical structure of indigenous asphaltenes..

The latter strategy has received special attention during the last ten years as a fundamental approach to understand the physical behavior of indigenous asphaltenes in terms of aggregation, adsorption, desorption and other interfacial properties by establishing similarities and differences through various experiments and simulations. The "Archipelago" and "Continental" models for asphaltenes have been traditionally used to attempt a description of a general structure for asphaltenes. In the former, several aromatic sections are attached to each other via alkyl chains. In the latter, polycyclic aromatic hydrocarbons (PAHs) form a core to which aliphatic chains are attached[28, 29]. The work of Groenzin and Mullins[30, 31, 32] shows strong evidence that points towards the validity of the continental over the archipelago model for asphaltenes.

Numerous works on model compounds have been presented following primarily the continental model with little studies based on the Archipelago model. A recent review[24] on the up-to-date literature highlighted a number of these studies. Akbarzadeh et al.[33] studied the self-association properties (aggregation number and stability of aggregates in solution) of a series of derivatives of the four-ring component, pyrene. These properties were significantly different than those of the indigenous asphaltenes in similar solutions concluding that the pyrene-based compounds proposed lack core features that represent real systems.

Rakotondradany et al.[34] studied the self-association properties of a model compound based on alkyl hexabenzocoronenes. Their study showed that even at concentrations as high as 15 g/L the model compound tends to form dimers, not found in indigenous asphaltenes. Tan et al studied the self-association, cracking and coking properties of archipelago pyrene-based model compounds[35, 36]. The authors found that the compounds self-associate due to π-π stacking interactions involving the pyrene rings and the bypiridine spacer and that the model compounds in the presence of heteroatoms exhibited coke yields comparable to hydrocarbon compounds. Molecular dynamic simulations (MDS) performed by S. Bhattacharjee and J. Masliyah[37, 38] using different model compounds (archipelago, continental and anionic continental) showed that molecules with charged terminal groups are tethered to the toluene-water interface whereas uncharged compounds were not observed to adsorb in the simulations. Additionally, they found that polyaromatic rings are stacked and perpendicularly inclined to the same interface.

The research by Sjöblom and coworkers[39, 40] on model compounds consisting of a polyaromatic core (perylene-based) with a fixed hydrophobic part in one side and branched alkyl chains of varying end-groups (acidic-end or aliphatic-end) in the other, showed that several features of indigenous asphaltenes can be mimicked. In particular, the model compound C5Pe exhibited similar solubility in heptane-toluene mixtures and similar interfacial tension concentration dependence when compared to indigenous asphaltenes. Studies at the water-air interface using Brewster Angle Microscopy (BAM) suggest that the polar groups adopt a *head-on* conformation with a face-to-face packing of the core. That is, the polar head (acidic group) prefers the aqueous phase and the polyaromatic cores stack normal to the surface.

A better and thorough understanding of sorption and rheological aspects of asphaltenes is needed. Hence in this work, a detailed study based on model compounds at the liquid/liquid and liquid/air interface is proposed and their properties are compared to the behavior of indigenous asphaltenes described in the up-to-date literature. The advantage of the model system is that it could be used to create very well defined and reproducible interfaces, which is often a problem with indigenous asphaltenes due to presence of aggregation phenomena which may introduce a dependency on time and preparation procedures. In the present work, a series of pendant drop and shear rheology experiments are performed not only to achieve this goal but also to serve as an example of the importance of distinguishing between processes driven by surface/interfacial tension (adsorption/ desorption) that give rise to an

apparent elasticity and processes dominated by extra deviatoric stresses that provide true linear viscoelastic moduli, material functions and elasticity in the rigorous sense. Although the system chosen for this work is aimed to establish more realistic model systems that resemble aspects of indigenous asphaltenes, the results can be extended to other colloidal systems.

2. Experimental section

Solvents and chemicals.

12-tricosanone (97%), used as the starter for model compound synthesis and n-heptane (for analysis Emsure Reag. PhEur) were purchased from VWR-Norway. Toluene (99.8%) anhydrous used to prepare all the model compound solutions and other chemicals necessary for synthesis were purchased from Sigma-Aldrich. All chemicals were used as received with no further purification.

Asphaltene model compounds.

Two asphaltene model compounds were used for this work. The first one, named C5PeC11, has an acidic functionality. The second one, named BisAC11 has little to no interfacial activity. C5PeC11 was synthetized by following the 4-step procedure described in Nordgård et al.[40] and Holman et al.[41] and by replacing 7-tridecanone with 12-tricosanone. 12-tricosanone is first treated with ammonium acetate and sodium cyanoborohydride in isopropyl alcohol to convert it into its corresponding amine. The amine is then reacted with perylene-3,4,9,10-tetracarboxylicdianhydride in the presence of imidazole. This step yields BisAC11 as an intermediate product. BisAC11 is further treated with potassium hydroxide in tert-butanol to obtain a monosubstituted intermediate. This compound is then reacted with 6-aminohexanoic acid in imidazole. Fig. S1 of the supporting information provides the chemical structure and the molar mass of the model compounds of this study.

Intermediate and final products were characterized by ^{1}H NMR spectroscopy in CDCl$_3$. All the peaks are accounted for and yield a match with the expected chemical structure; hence the purity of these compounds is assumed to be very good. C5PeC11 was purified by flash chromatography on silica gel using a methanol-chloroform mixture (0-5% in CHCl$_3$) as eluent. BisAC11 was purified by contact with silica particles (Aerosil 200) for 24h to remove any surface active impurities.

Water phase. The water phase for adsorption/desorption measurements and for dilatational rheological measurements was a buffer solution of pH 8 prepared with Mili-Q water (resistivity of 18.2 MΩ·cm) and 0.1M KH_2PO_4 adjusted with 0.1M NaOH solution. The water phases for the compression-expansion curves and shear rheology experiments were buffer solutions of pH 5 (0.2M $CH_3COONa \cdot 3H_2O$ adjusted with 0.2M CH_3COOH), pH 6 (0.1M KH_2PO_4 adjusted with 0.1M NaOH) and pH 8 (0.1M KH_2PO_4 adjusted with 0.1M NaOH) prepared with Mili-Q water.

Interfacial tension, dilatational rheology and desorption measurements.

A commercially available sessile/pendant drop tensiometer (PAT 1m, SINTERFACE Technologies, Berlin, Germany) was used. This instrument determines the surface/interfacial tension of a surfactant-covered liquid droplet (or air bubble) by recording its silhouette onto a CCD camera. The digital images are then analyzed and fitted to the Young-Laplace equation with an accuracy of ±0.1mN/m. This equation relates the curvature of a liquid drop and the surface/interfacial tension. The built-in software produces a series of theoretical curves by changing the values of the surface/interfacial tension. The curve that yields the best fit to the experimental points is then used to report the measured surface/interfacial tension. For this procedure, only the densities of the oil and aqueous phase are needed. This technique is also known as axisymmetric drop shape analysis (ADSA). It is important to note that for systems dominated by surface/interfacial tension (adsorption/desorption) as, for instance, the present study, the contributions of extra mechanical stresses are negligible thus the Young-Laplace equation remains valid. However, for systems in which these deviatoric stresses are not negligible (for example asphaltenes that are known to form an elastic interfacial skin) the validity of the equation is questionable.

Desorption experiments were performed with a previously used[42, 43] accessory to the tensiometer that consists of two concentric capillary tubes (a schematic is shown in Fig. S2 of the supporting material). Material can be pumped or withdrawn independently by two automatic pumps. An oil droplet (e.g. C5PeC11 droplet in toluene) is formed at the tip of an outer capillary with one automatic pump and the droplet is allowed to equilibrate for a fixed period of time ($t_0 = 30\ min$) inside a cuvette (25 mL) that contains the aqueous solution (pH 8 buffer). The volume of the droplet is $V_D = 18\ \mu L$. This particular equilibration time was chosen for practical reasons and because the equilibrium interfacial tension did not change even after 6h. After the fixed equilibration time, the convection-driven subphase exchange

inside the well-mixed droplet begins. The subject solution (toluene, HepTol or BisAC11) is injected through an inner capillary controlled by the second pump at a given volumetric flow rate ($Q = 0.4 \, \mu L/s$). During this stage, the droplet volume is kept constant at $V_D = 18 \, \mu L$ through simultaneous withdrawal from the outer capillary using the first pump and video feedback control. Once the total predetermined volume ($V_E = 1000 \, \mu L$) has been exchanged, pumping/withdrawal stops. The IFT then reaches a plateau value. This process takes exactly $V_E/Q = (1000 \mu L)/(0.4 \mu L/s) = 2500 s$. The interfacial tension is continuously measured during all stages of the experiments. The plots regarding desorption experiments correspond to the average of two duplicates and only the IFT-time lapse of the desorption stage is shown (2500s, that is from t_0 until V_E has been exchanged) as a function of the characteristic time ($(Q(t' - t_0))/V_D$ or simply Qt/V_D) where t' corresponds to the total time . To avoid handling a large number of experimental points, a 2 s moving average was used. All experiments were performed by duplicate at 22°C and the experimental conditions were set up based on our previous studies[42, 43]. Additional details on the technique can be found elsewhere[44, 45].

Interfacial dilatational rheology measurements were automatically started after the fixed equilibration time of 30min. Once again, the volume during the oscillations is controlled by the software via constant feedback. Five cycles at five different frequencies were performed using an amplitude of 7% (18 ± 1.26 µL). The five frequencies were 0.01, 0.013, 0.02, 0.04 and 0.1 Hz.

Langmuir trough experiments

Compression-expansion curves performed at a liquid-air interface and at a liquid-liquid interface were also completed in Langmuir troughs (KSV Instruments Ltd. Finland) with dimensions of 75 x 330 mm and 65 x 260 mm, respectively. Experiments were performed at 22°C, and a platinum Wilhelmy plate with a perimeter of 39.44 mm attached to a Wilhelmy balance (KSV Instruments Ltd. Finland) was used to measure surface tension. All compression-expansion experiments were performed at a constant rate of 3 mm/min.

Interfacial shear rheology.

Shear rheological measurements were performed with a double wall ring (DWR) geometry[46] attached to a Discovery HR-3 rheometer (TA Instruments). The ring is 7 cm in diameter with a thickness of 1mm and was produced with additive manufacturing (Layerwise, Leuven) from titanium (Ti6Al4V Grade 5). The cross section of the ring is square and rotated 45

degrees such that two corners sit in the interfacial plane and pin the interface to the geometry. There are 3 evenly spaced openings in the ring to facilitate a homogeneous distribution of interfacial material inside and outside the confines of the ring geometry[47]. The cup geometry is Teflon and can be placed within the Langmuir trough. The cup has two openings to allow the interfacial coverage to come to equilibrium inside and outside the cup perimeter, and it has a 0.5 mm deep step on the inside of the cup to pin a horizontal interface. The distance between the inner and outer walls at the point of pinning is 8 mm. Surface shear viscosities of approximately 10^{-5} Pa.s.m can be resolved with this setup and this geometry. Since these experiments are performed at constant area and with well-defined kinematics, extra stresses originate solely from the deformation of interfacial structure and can be related to proper material functions.

3. Theory

Theoretical considerations can be divided in three stages: (1) interfacial tension data (2) Apparent interfacial dilatational elasticity and apparent elastic modulus modeled using the approach proposed by Lucassen-van den Tempel[23] and (3) extra stresses probed by interfacial shear rheology and the soft glassy rheology model (SGR)[48].

Langmuir Isotherm.

Equation (1), is a two parameter equation which assumes that there are no interactions between the adsorbed species and that the molecules are reversibly adsorbed as a monolayer. The analogous equation of state (2) is known as the Szyszkowski equation, as reported by Chang and Franses[49].

$$\Gamma = \Gamma_\infty \left(\frac{K_L c}{1 + K_L c} \right) \tag{1}$$

$$\pi = nRT\Gamma_\infty Ln(1 + K_L c) \tag{2}$$

In these equations, Γ is the surface coverage, Γ_∞ is the surface excess at the saturation point, K_L is commonly known as the adsorption equilibrium constant, π is the difference in interfacial/surface tension between a freshly formed interface/surface and the value at a given concentration of surface active species, c is the bulk concentration and n is a parameter that accounts for the adsorption of counter-ions. In this case this parameter is equal to one[49].

A desorption model based on equations (1) and (2) was established by Svitova et al.[50] for the convective-type of flow present in a coaxial capillary. They proposed equation (3) to be used in equation (2) and successfully described desorption of non-interacting and reversibly adsorbed species under convection flow. Pradilla et al.[42] used this model to successfully describe desorption of simple surfactants at the liquid-liquid and liquid-air interface.

$$C = C_0 exp(-Qt/V_D) \tag{3}$$

In this equation, C is the evolution of the concentration inside the drop during desorption, C_0 is the initial bulk concentration, Q is the volumetric flow rate, t is the time of the desorption stage and V_D the volume of the droplet.

Interfacial dilatational rheology.

Axisymetrical drop shape analysis (ADSA) has been recognized as a reliable method for measuring adsorption/desorption dynamics and the compressibility of the interface[51, 52], and provided that the contributions of extra mechanical stresses are negligible, it is an accurate method for interfacial tension experiments.

The principle behind the oscillating drop is that the interfacial tension varies when the area (A) of a droplet is changed in an oscillatory manner at a given frequency (ω) from an initial (A_0) to a value (A_a) following equation (4)[53].

$$\Delta A = A - A_0 = A_a \sin(\omega t) \tag{4}$$

The complex dynamic apparent dilatational modulus (E^*) is then typically defined as the Fourier transform ($\mathcal{F}$) of the change in interfacial tension (γ) relative to the change in interfacial area via equation (5)[54]. The complex modulus can also be interpreted by a real and an imaginary part. The real part characterizes the elastic properties of the interfacial layer and the imaginary part characterizes the viscous properties. These parts are referred as to the apparent elastic dilatational modulus E' and the apparent viscous dilatational modulus E''.

$$E^*(\omega) = \frac{\mathcal{F}\{\Delta\gamma(t)\}}{\mathcal{F}\{\Delta\ln(A(t))\}} = E'(\omega) + iE''(\omega) \tag{5}$$

Lucassen and van den Tempel[23] proposed a model for the variation of the elastic and viscous dilatational moduli as a function of the concentration (c) which is only valid for flat surfaces. The main underlying assumption of this model is that the adsorption is diffusion-controlled. In this model, the elastic and viscous components of the complex modulus depend on the independent contributions of the so called Gibbs elasticity ($E_0 = \Gamma(d\gamma/d\Gamma)$) which characterizes the compressibility and a parameter that accounts for diffusion defined as: $\Omega = \sqrt{D/2\omega}(dc/d\Gamma)$ in which (D) is the diffusion coefficient. The apparent elastic and viscous dilatational moduli are therefore calculated using equations (6) and (7).

$$E'(\omega) = E_0 \frac{1 + \Omega}{1 + 2\Omega + 2\Omega^2} \tag{6}$$

$$E''(\omega) = E_0 \frac{\Omega}{1 + 2\Omega + 2\Omega^2} \tag{7}$$

Equation (6) and Equation (7) provide apparent moduli and not true material functions. It has been recently shown[54] how the curvature of the droplets will influence the measured apparent moduli. This is due to its impact on mass transport: the mass flux will be higher near a highly curved interface compared to the planar case. Additionally, for systems in which extra stresses are significant, these effects are unaccounted for in the classical analysis for pendant drop experiments and dilatational rheology measurements[53].

Interfacial shear rheology.

A model which describes the rheology of crowded systems in which rearrangement of internal structure is difficult is the soft glassy rheology (SGR) model[48]. This empirical model predicts rheological behavior of soft materials with meta-stability and structural disorder at high concentrations. A soft glassy material has time and frequency dependent viscoelastic properties, and the SGR describes this dependence in terms of an effective noise temperature. This effective noise temperature is indicative of the ability of a disordered, metastable microstructure to rearrange, and depends on internal microstructure and flow history. Thus, small values of effective noise temperature would indicate a highly arrested system, while large values indicate a system that will readily flow. For an effective noise temperature with a value between one and three the SGR model predicts[48]:

$$G' \propto \omega^{x-1} \text{ for } 1 < x < 3 \tag{8}$$

$$G'' \propto \omega^{x-1} \text{ for } 1 < x < 2 \tag{9}$$

where x is the effective noise temperature, ω is the frequency, and G' and G'' are the storage and loss moduli respectively. For an effective noise temperature between one and two the model predicts a viscoelastic response with shear-thinning behavior and the same scaling of G' and G'' with ω. An effective noise temperature less than one indicates a glassy system with arrested dynamics [48]. The SGR model has been used to describe interfacial rheological properties in polymers at an air/water interface [55], rough carbon black particles at a water/n-octane interface [56], and indigenous asphaltenes at a water/hexadecane interface [12].

4. Results and discussion

4.1 Adsorption and desorption dynamics.

Adsorption isotherm. Before determining the adsorption isotherm of C5PeC11, the influence of the pH on the equilibrium (30 min) interfacial tension at a fixed concentration (0.05mM) was assessed. This was done not only to show the influence of the acidic functionality of the molecule, but also to choose a suitable pH for the rest of the experiments. Fig. 1 shows that lower pH values do not strongly influence the equilibrium IFT. There is a sharp transition at pH 6, and IFT values decrease rapidly with increasing pH. At pH values greater than 9 it was not possible to generate a stable droplet for measurement, which suggests very low IFT values (<1-2 mN/m). Based on these observations, pH 8 was chosen as the water phase for the rest of the experiments of this work. The interesting aspect of Fig. 1 is that this behavior is similar to C_6-asphaltene solutions in xylene at 0.1 g/L reported by Nenningsland et al.[22] when compared to the neutral and basic media.

The interfacial tension after an equilibrium time (aging) of 30 min as a function of the bulk concentration of C5PeC11 solutions in toluene is presented in Fig. 2. After the aging time, the changes in IFT were less than 0.2 mN/m, thus equilibrium was attained. The solid line represents the fit to the Langmuir equation of state (EoS). The equilibrium parameters obtained via equations (1) and (2) are also shown. The surface excess for this molecule was found to be $\Gamma_\infty = 2.26 x 10^{-6} mol/m^2$ which yields a mean molecular area at maximum coverage of $Mma = 73.46 \text{ Å}^2/molecule$. Nordgård et al. [39, 57] measured the mean molecular area after adsorption onto silica particles and the limiting area (A_0) on a surface-pressure

isotherm at the liquid-air interface of a similar model compound, namely C5Pe. They reported the values 120 and 46 $Å^2/molecule$ which are consistent with a *head-on* arrangement of the molecule at the interface. Taking these values into account, this means that the asphaltene model compound C5PeC11 adsorbs most likely perpendicular to the interface with the acidic group into the water phase and the rest of the molecule into the oil phase. The surface-pressure isotherms of the upcoming sections will go into further details about the conformations at the interface.

All the assumptions behind the Langmuir EoS are not necessarily met, especially since the system C5PeC11/Toluene does not exhibit complete reversibility of adsorption as it will be shown in later sections. However, from a semi-quantitatively point of view, the equilibrium parameters are of the same order of magnitude to those obtained by Pradilla et al.[43] for C_6-asphaltene solutions in xylene ($K_L = 228 \, m^3/mol$ and $\Gamma_\infty = 9.54x10^{-7} mol/m^2$) and a demulsifier of similar molecular weight ($K_L = 834 \, m^3/mol$ and $\Gamma_\infty = 1.06x10^{-6} mol/m^2$). These values give a semi-quantitative notion of their surface activity and are only valid as long as the area is kept constant. When compression/expansion occurs, the equilibrium parameters evidently change.

Interfacial dilatational rheology. The influence of pH on the apparent elastic dilatational modulus measured after an equilibration time of 30min is also presented in Fig. 1 for two different frequencies. The apparent elastic modulus increases when the pH increases and tends to reach a plateau at high pH values. Similar results were obtained when the equilibration time was changed to ~6h (results not shown). This behavior was expected because of the acidic nature of the molecule. The important aspect of this trend is that it is very similar to that reported for C_6-asphaltene solutions in xylene under similar conditions[22]. They obtained an increase of the apparent elastic dilatational modulus from ~10 to ~25 mN/m when the pH changed from 6 to 12 under similar experimental conditions. The values however are always higher for asphaltenes due to the known phenomenon of the formation of a mechanically robust film at the interface (skin). This could indicate that the acidic functional groups present in asphaltenes are largely responsible for the interfacial behavior at liquid-liquid interfaces[58].

To test the system C5PeC11/Toluene for skin formation, a series of droplet contraction/expansion qualitative experiments similar to those performed by Jeribi et al.[7] were done on C5PeC11 droplets. First, a droplet of C5PeC11 in toluene is formed at the tip of

a capillary. Second, the droplet is aged for a fixed amount of time; in this case, 30 min. And third, the droplet is contracted and expanded rapidly, changing the volume up to 60% of the original value. In the case of asphaltene solutions in toluene reported by Jeribi et al.[7], the "skin" is clearly visible as well as droplet distortion after the given aging times (crumpling). Additionally, after the contraction/expansion cycles, the original shape of the droplet was never recovered. These remarks were explained through asphaltene multilayer formation and the irreversibly adsorbed nature of the asphaltene rigid layer. Fig. S3 of the supporting material shows the contraction/expansion experiments for C5PeC11 solutions in toluene and there is no indication of skin formation, even after 5 consecutive cycles the shape after compression remained the same and the Young Laplace equation fitted it well. This does not mean extra stresses are absent, but it indicates that the response to dilatational deformations is dominated by interfacial tension and its variations.

Fig. 3a and 3b show the evolution of the apparent elastic and viscous dilatational moduli as a function of the concentration of C5PeC11 solutions in toluene after an equilibration time (aging) of 30 min. The apparent moduli were measured at five different frequencies ranging from 0.01 to 0.1 Hz. These frequencies were chosen to compare the results obtained with the model compound to those reported in the literature for asphaltenes of different sources[18, 19, 21, 22]. The general trend of the curves to shift towards areas of lower apparent elastic (and viscous) modulus as the frequency decreases. This behavior is expected because at low frequencies (0.01 Hz), the expanding interface is exposed to the bulk for longer times allowing diffusion mechanisms to restore the surface tension to its equilibrium value. At high frequencies the timescale of the deformation is fast compared to the diffusive time scale and changes in area lead to variations in surface tension that are picked up in the measurement as an apparent elasticity[18]. An important feature of Fig. 3 is that the apparent moduli increase as a function of concentration, congruent with the increase in Gibbs elasticity (E_0). At high concentrations (>0.05 mM), after a maximum, both contributions decrease and reach a plateau. This behavior is precisely what has been observed for asphaltenes[21] and crude oil solutions[20]. Care should be taken here when interpreting the data. Although the trends in the apparent elastic and viscous moduli are similar between asphaltenes and C5PeC11, adsorption features are different. Where asphaltenes are known to irreversibly adsorb at the liquid-liquid interface with subsequent multilayer stacking and "skin" formation, which influences the Young Laplace equation fit, C5PeC11 does not form such a skin. The results in

the next section strongly suggest that the relaxation of C5PeC11 is almost purely diffusional, and that the observed effects can be attributed to changes in surface tension.

Fig. 3 also shows the fits of the apparent elasticity using the LvdT model for C5PeC11 solutions in toluene at different frequencies and bulk concentrations. The fitting procedure is performed assuming that the Langmuir EoS remains valid which allows setting $E_0 = \Gamma_\infty K_L cRT$ for each concentration taking the values from Fig. 2. In this way, the parameters Ω and ω present in equation (6) and equation (7) are fixed. This leaves the diffusion coefficient D as the only variable to be adjusted to the best match of the experimental data. Fig. 3a and 3b show the best fit to the elastic and viscous dilatational moduli respectively, with a diffusion coefficient (which is the material property underlying the phenomena) of $4\text{x}10^{-10}$ m^2/s. This value for the diffusion coefficient is comparable to those reported by Chang et al.[59] for molecules of similar molecular weight. Although the predictions of the model are not perfect, they describe the evolution qualitatively, especially in the vicinities of the maxima, which are well predicted, and the decrease of the moduli at higher bulk concentrations. This suggests that C5PeC11 adsorption governs the phenomena, and that this is reversible, a fundamental assumption underpinning the LvdT model. It was also shown that there is no skin (or crumpling) preset at the interface even at long aging times and that thermodynamic equilibrium between interface and bulk was attained. The adsorption of C5PeC11 is almost completely reversible, meaning that after desorption experiments the interfacial tension of pure toluene/water is almost achieved. The small portion of C5PeC11 that remains at the interface could explain the prediction differences of the LvdT model.

Different attempts have been reported in the literature to improve the fit of the interfacial dilatational rheology data of indigenous asphaltenes[17, 18, 19, 20, 22] using the LvdT approach and assuming different mathematical variations of the asphaltene diffusion coefficient with concentration. The assumed diffusion coefficients are generally low ($1\text{x}10^{-11}$ m^2/s - $1\text{x}10^{-10}$ m^2/s [21] or $1\text{x}10^{-18}$ m^2/s - $2\text{x}10^{-12}$ m^2/s [42]). However, LvdT is not a general model describing the response to interface deformations, as it describes only the response to variations of the surface tension governed by the Gibbs elasticity and the time scale of transport to and from the interface. In the case of asphaltenes there are several other effects that may contribute. First, asphaltene adsorption is almost irreversible[43]. Secondly, extra stresses inherent to the interface are not accounted for in the LvdT model[54]. Also multilayer formation may occur which will influence the response to changes in area. In this sense, there is a fundamental difference between the behavior of indigenous asphaltenes and the asphaltene model

compound C5PeC11. Even though several aspects of interfacial dilatational rheology, in particular those related to changes in surface tension, are similar and can be used to make predictions about the stability of the equivalent emulsions, some phenomena are not present in C5PeC11 adsorption, especially that of skin formation.

Desorption from the liquid-liquid interface. This section deals with the study of desorption of the asphaltene model compound C5PeC11 from the liquid-liquid interface by means of three different substances: desorption of the model compound by pure solvent (in this case toluene) is first presented, followed by desorption by a mixture of heptane and toluene (HepTol) close to the precipitation onset, ending with desorption induced by the model compound BisAC11. This was achieved using a double-capillary system (Fig. S2 of the supporting material) accessory to the ADSA instrument. This system has been previously used to study desorption of asphaltenes and model demulsifiers, hence details on how it works can be found elsewhere[42, 43].

Fig. 4 shows a plot of the interfacial tension as a function of the dimensionless characteristic time (Qt/V_D) for desorption of C5PeC11 at three different concentrations induced by toluene. For comparison purposes, a desorption model based on the Langmuir isotherm is also included (partly obtained from equation (3)). This model has been shown to adequately describe desorption of non-interacting reversibly adsorbed species at the liquid/air[50] and liquid-liquid[42] interface. However, desorption of C5PeC11 is slower than the prediction which suggests the presence of interactions at the liquid/liquid interface among the model compound. These interactions, which are rather weak to be detected by dilatational experiments dominated by surface tension changes, are most likely due to intermolecular forces such as hydrogen bonding and π-π stacking of the core as it will be shown in later sections. From the desorption experiments it could be possible, in principle, to calculate a convective mass transfer coefficient. However this goes beyond the scope of this article.

The data in Fig. 4 suggest that the adsorption is almost fully reversible. Comparing the final value of the interfacial tension after desorption, γ~33mN/m, and the value for toluene/aqueous solution, γ~36mN/m, it can be concluded that there is some material that remains irreversibly adsorbed at the interface (within the time scales of the experiment). Fig. 5 shows similar data, but desorption is now induced by a mixture of heptane-toluene or, "HepTol" at 30/70 (%v/v) and the model compound BisAC11 has an aliphatic end group. The filled symbols in Fig. 4 show that when using a HepTol mixture that is close to the

precipitation onset of the asphaltene model compound, the degree of desorption is the same as that of toluene (open symbols). It is important to highlight that C5PeC11 was dissolved in the same HepTol mixture for this curve (filled symbols). From this it follows that the reversible nature of adsorption of C5PeC11 onto the liquid-liquid interface is not related to its solubility. Even in a poor solvent (HepTol), desorption was the same as in a good solvent (pure toluene). Extrapolating this idea to asphaltenes, which also precipitate in HepTol solutions at volume fractions ~30/70% and ~40/60%[60], it could be hypothesized that the irreversibility in their adsorption is not related to their poor solubility but instead to other mechanisms such as changes in conformations and π-π interactions at the interface. Strong interactions might be responsible for the observed delay in desorption when comparing with a non-interacting model (Fig. 4) which was also previously observed for asphaltenes[42].

Fig. 5 contains data on the desorption curves of C5PeC11 at a fixed concentration of 0.1mM induced by the asphaltene model compound BisAC11, which has an aliphatic end group. Two concentrations of BisAC11 were chosen: a lower concentration of 0.05mM and a higher concentration of 1.74 mM which is roughly 20 times greater than that of C5PeC11. The model compound BisAC11 has little to no influence on the desorption of C5PeC11 suggesting that there are little to no interactions between these two model compounds. More importantly, the delay in C5PeC11 desorption that occurs between $Qt/V_D \sim$ 0-15 and the final values of the interfacial tension γ~33 mN/m indicate that the portion of irreversibly adsorbed C5PeC11 does not interact with BisAC11 at the liquid-liquid interface. The small decrease in the interfacial tension that occurs at a high concentration of BisAC11 after $Qt/V_D \sim 25$ is attributed to surface active impurities that accumulate at the interface and the low surface active nature of BisAC11 that could potentially displace small portions of C5PeC11 or fill empty pockets created by desorption of large aggregates. To emphasize this point, the equilibrium interfacial tension of BisAC11 in toluene was measured at pH 8 and found it to be γ~ 34.5 mN/m suggesting, once again, low to no interfacial activity of this compound. This type of minor interactions between C5PeC11 and BisAC11 at the liquid/liquid interface could be comparable to that of acidic and non-acidic components of crude oil that exhibit a similar behavior in terms of interfacial tension[61].

4.2 Extra stresses as probed by shear rheology.

At an air/water interface C5PeC11 behaves as an insoluble Langmuir film. Although the behavior of an interfacially active material at an air/water interface is expected to be

significantly different than at an oil/water interface, one can learn a great deal about certain aspects of interfacial behavior, such as the tendency to aggregate. Model molecules at an air/water interface may display certain features characteristic of skin-forming asphaltenes.

In Fig. 6a a series of compression-expansion curves for C5PeC11 at an air/water interface and a pH of 6 are shown. Cycles of compression-expansions were consecutive, the first of which began 30 minutes after spreading C5PeC11 from toluene. The first compression curve in Fig. 6a is different than all of the following compression curves, and has a local maximum at a molecular area of approximately 90 $Å^2$/molecule. This bump in the curve is a non-thermodynamic behavior that appears at a molecular area consistent with the molecules of C5PeC11 at monolayer coverage and with a strong tilt. The competing dynamics involved are the continuous compression of the interface and the slow dynamics associated with rearrangement of the molecules at the interface as they become increasingly confined. The local maximum in the curve is present only in the first compression, suggesting that the initial state of the interface is dependent on the initial solvent spreading and evaporation history. After the first compression-expansion, consecutive curves in Fig. 6a look similar but continue to shift to lower values of molecular area with each compression-expansion. In an insoluble system this behavior is indicative of irreversible aggregate formation at large surface pressures and the formation of multilayers. Evidence for the surface-pressure dependence of aggregate formation is seen in Fig. 6b, where consecutive compression-expansion curves are shown but the surface pressure never exceeds 30 mN/m (i.e. a surface pressure lower than the collapse value). At low surface pressures, after the first compression, consecutive compression-expansion curves are repeatable and indicate that aggregate formation is strongly surface-pressure dependent. Data in Fig. 6 suggest that C5PeC11 has a slow dynamic associated with molecular rearrangements at monolayer coverage, and at high surface coverage there is a driving force toward irreversible aggregation and the formation of multi-layer structures[62].

Rheological behavior is coupled to material microstructure, and the rheological data shown in Fig. 7 is indicative of a material with elastic, fragile microstructure. In Fig. 7a storage and loss moduli are plotted as a function of strain at 30 mN/m. The deviation from a linear viscoelastic regime begins at relatively small strain values of 0.2 to 0.5%. The structures which dominate the transfer of stress through the interface are easily ruptured. Frequency sweep data obtained at 0.1% strain is shown in Fig. 7b and reveals that a broad range of relaxation times are present in C5PeC11 at the air/water interface. The values of the storage

moduli show that significant elasticity is present at the interface, as expected for a strongly interacting insoluble system.

The behavior of C5PeC11 at the oil/water interface is more relevant for comparison to indigenous asphaltene behavior in crude oil emulsions and the data presented in the previous sections. Compression-expansion curves from C5PeC11 at a decane/water interface are shown in Fig. 8. Prominent in the compression curves is the non-thermodynamic local maximum that was also observed in the first compressions in Fig. 6. In Fig. 8 the molecular area at which this peak is found is 65-70 Å^2/molecule. This is a smaller value than that found for the air/water interface in Fig. 6, and it can be explained in terms of the tilt of the molecules at the interface. With an oil phase, it would be expected that the hydrocarbon tails and aromatic groups of C5PeC11 would preferentially immerse in the oil phase, resulting in less tilt and a smaller molecular area at monolayer coverage. Unlike the air/water interface, the peak is observed on all consecutive compressions at the decane/water interface. The presence of oil makes the dynamics of molecular rearrangement reversible, and indicates the nature of the rearrangement; indigenous asphaltenes have the ability to undergo π-π stacking and one might expect to observe similar behavior in C5PeC11 because of the prominent aromatic groups at the core of the molecule. The local maximum observed may be the competition between compression of the interface and the dynamics associated with the formation of π-π stacks and rearrangement of the resulting domains. The reversibility of this behavior at an oil/water interface may be attributed to the ability of decane molecules to re-insert between molecules at low surface pressure, reversibly destroying bonds associated with π-π stacking upon expansion of the interface. Although all compression-expansion measurements were made at a barrier movement rate of 3 mm/min, it is worth noting that the soluble nature of these molecules in the oil phase is expected to result in a dependence on compression rate that might affect both the hysteresis behavior and the non-thermodynamic local maximum observed during compression. The results are consistent with the data obtained in the pendant drop experiments.

Shear flow at a constant area isolates the mechanical response of the interfacial structure in the absence of adsorption/desorption dynamics. In this way the material functions give rise to the extra stresses generated at the interface and can be measured. Results for C5PeC11 at the decane/water interface at 30 mN/m are shown in Fig. 9. The linear viscoelastic regime is small, similar to the behavior observed in Fig. 6a for the air/water interface and again indicative of fragile structures. Storage and loss moduli as a function of frequency were

obtained at a strain of 0.1%, and are shown in Fig. 9b. The magnitudes of the moduli are smaller than those for the water-air interface, and rather small. The frequency dependence reveals a viscoelastic structure with a broad range of relaxation time. This rheological behavior is characteristic of a soft-glassy material, where rearrangement under flow of a densely packed internal structure takes place with a broad range of characteristic times. The straight lines plotted in Fig. 9 come from fitting the soft-glassy rheology (SGR) model to the linear viscoelastic data in Fig. 9b. An effective noise temperature of 1.34 was obtained from the fit, and the prediction of the SGR model of the scaling of G" in the non-linear regime is plotted in Fig. 9a. A value of the effective noise temperature between one and two is indicative of a soft-glassy rheological response with storage and loss moduli that both vary with respect to ω^{x-1}. This behavior is characteristic of what is found in indigenous asphaltenes at surface concentrations sufficient to stabilize oil and water emulsions[12, 63]. A comparison of effective noise temperature measured here and values measured in indigenous asphaltenes by Samaniuk et al. [12] reveals that indigenous asphaltenes form a more arrested interface. Values of effective noise temperature between 1.3 and 1.4 were obtained in indigenous asphaltenes at surface pressures between 13 mN/m and 14 mN/m, and continued to decrease (indicating an increasingly arrested system) at higher surface pressures. The 1.34 value found here in the model molecule system was obtained at a high surface pressure of 30 mN/m, indicating that higher surface pressures are required in order to obtain the same effective noise temperature values observed in indigenous asphaltenes. This results in smaller extra stresses developing in the interface when deformed, which is in agreement with the absence of significant elastic effects contributing in the dilatational measurements. Although indigenous asphaltenes are a complex mixture of many molecules that form hierarchic structures, we have found here that it is nevertheless possible to capture important characteristics of their rheological behavior with model molecules of a single chemistry and architecture.

The influence of pH on the stabilizing effect of indigenous asphaltenes is significant, and pH modification has been considered as a strategy for emulsion breaking[64]. Compression curves for C5PeC11 at a decane/water interface are shown in Fig. 10a for three different subphase pH values. With the subphase at a pH of 8 the carboxylate functional group of C5PeC11 is highly deprotonated and expected to be more surface active than at lower pH. In addition to increased surface activity, a decrease in the tilt of the molecule at the interface is expected. This is seen in Fig. 10a as a shift of the location of the local maximum in the compression

curve to lower values of molecular area. The value of 66 Å^2/molecule is at the low end of the range of values obtained from similar particles adsorbed onto silica[57], and consistent with a very upright orientation of the molecule at the interface. An illustration of this arrangement is shown in Fig. 10b, where the tilt-state of the C5PeC11 is expected to depend on the state of the carboxylate functional group. As the pH is decreased the carboxylate group becomes more protonated, less charged, and less surface active. At a pH of 5 the surface activity decreased significantly and the local maximum in the compression curve shifted to a molecular area of 105 Å^2/molecule, consistent with a highly tilted orientation of the molecules of C5PeC11. The strong dependence of the interfacial activity of C5PeC11 on pH is consistent with behavior observed in C$_6$-asphaltenes[22]. The carboxylate functional group on C5PeC11 captures important aspects of this behavior.

Conclusions

Sorption dynamics of C5PeC11, a model compound for indigenous asphaltenes, showed that it is essentially reversibly adsorbed at the toluene/water interface even under conditions near the precipitation onset (Fig. 4 and Fig. 5). Interactions between C5PeC11 and BisAC11 at the same interface were not observed, suggesting that alkyl end groups have little to no influence in asphaltene adsorption whereas polar interactions (-COOH groups) dominate this behavior. Unlike indigenous asphaltenes, C5PeC11 does not exhibit a macroscopic skin formation yet there is significant viscoelasticity and extra stresses observed in the shear measurements.. However, equilibrium parameters based on the Langmuir equation of state and interfacial dilatational rheological results are similar, suggesting that these model compounds can be systematically used to study separately the interfacial tension related effects of indigenous asphaltenes. Unlike for indigenous asphaltenes the responses observed in pendant drop experiments are dominated by surface/interfacial tension and mass transport phenomena.

At the air/water interface, where interactions are stronger, C5PeC11 shows a strong hysteresis between the first compression-expansion cycle and consecutive cycles that is indicative of an irreversible rearrangement of the molecules upon the first compression. Compression to large surface pressures results in a shift of the consecutive curves to smaller molecular areas, a sign of aggregation and the formation of multilayer structures. At a decane/water interface the rearrangement of molecules during compression is reversible upon expansion and is attributed to the ability of oil molecules to penetrate π-π stacking arrangements between C5PeC11 molecules. Soft-glassy rheological behavior is observed in C5PeC11, consistent

with behavior observed in indigenous asphaltenes at an oil/water interface, but the behavior is less pronounced, congruent with observations in the dilatational experiments. In addition to soft glassy rheology, C5PeC11 shows a strong pH dependence that is very similar to that observed in indigenous asphaltenes. Although indigenous asphaltenes are polydisperse structures that aggregate to form larger clusters, we have found that important characteristics of asphaltenes at an oil/water interface, such as the presence of interfacial viscoelasticity and pH dependence, can be captured with a single model molecule of a defined chemistry and architecture.

Acknowledgements

References

1. Speight, J. G. Chapter 11: Asphaltene Constituents. In *The chemistry and technology of petroleum*, 4th Edition ed.; CRC Press. Taylor & Francis group. : Boca Ratón, FL. , 2007, pp 315-344.
2. Mullins, O. C. The Asphaltenes. *Annual Review of Analytical Chemistry* **2011,** *4* (1), 393-418.
3. Hammami, A., Ratulowski, John. Chapter 23. Precipitation and Deposition of Asphaltenes in Production Systems: A Flow Assurance Overview. In *Asphaltenes, Heavy Oils, and Petroleomics*, Mullins, O. C., Sheu, E., Hammani, A., Marshall, A., Ed.; Springer, LLC, 2007.
4. Buckley, J. S. Asphaltene Deposition. *Energy & Fuels* **2012,** *26* (7), 4086-4090.
5. Gonzalez, D. L.; Vargas, F. M.; Hirasaki, G. J.; Chapman, W. G. Modeling Study of CO2-Induced Asphaltene Precipitation. *Energy & Fuels* **2008,** *22* (2), 757-762.
6. Kilpatrick, P. K. Water-in-Crude Oil Emulsion Stabilization: Review and Unanswered Questions. *Energy & Fuels* **2012,** *26* (7), 4017-4026.
7. Jeribi, M.; Almir-Assad, B.; Langevin, D.; Hénaut, I.; Argillier, J. F. Adsorption kinetics of asphaltenes at liquid interfaces. *Journal of Colloid and Interface Science* **2002,** *256* (2), 268-272.
8. Hannisdal, A.; Orr, R.; Sjöblom, J. Viscoelastic properties of crude oil components at oil-water interfaces. 1. The effect of dilution. *Journal of Dispersion Science and Technology* **2007,** *28* (1), 81-93.
9. Pensini, E., Harbottle, D., Yang, F., Tchoukov, P., Li, Z., Kailey, I., Behles, J., Masliyah, J., Xu, Z. Demulsification Mechanism of Asphaltene-Stabilized Water-in-Oil

Emulsions by a Polymeric Ethylene Oxide–Propylene Oxide Demulsifier. *Energy & Fuels* **2014**.

10.   Zhang, L. Y.; Xu, Z.; Masliyah, J. H. Langmuir and Langmuir-Blodgett films of mixed asphaltene and a demulsifier. *Langmuir* **2003,** *19* (23), 9730-9741.

11.   McLean, J. D.; Kilpatrick, P. K. Effects of Asphaltene Solvency on Stability of Water-in-Crude-Oil Emulsions. *Journal of Colloid and Interface Science* **1997,** *189* (2), 242-253.

12.   Samaniuk, J. R.; Hermans, E.; Verwijlen, T.; Pauchard, V.; Vermant, J. Soft-Glassy Rheology of Asphaltenes at Liquid Interfaces. *Journal of Dispersion Science and Technology* **2015,** *36* (10), 1444-1451.

13.   Verruto, V. J.; Le, R. K.; Kilpatrick, P. K. Adsorption and Molecular Rearrangement of Amphoteric Species at Oil−Water Interfaces. *The Journal of Physical Chemistry B* **2009,** *113* (42), 13788-13799.

14.   Fan, Y.; Simon, S.; Sjöblom, J. Interfacial shear rheology of asphaltenes at oil–water interface and its relation to emulsion stability: Influence of concentration, solvent aromaticity and nonionic surfactant. *Colloids and Surfaces A: Physicochemical and Engineering Aspects* **2010,** *366* (1–3), 120-128.

15.   Spiecker, P. M.; Kilpatrick, P. K. Interfacial rheology of petroleum asphaltenes at the oil-water interface. *Langmuir* **2004,** *20* (10), 4022-4032.

16.   Harbottle, D.; Chen, Q.; Moorthy, K.; Wang, L.; Xu, S.; Liu, Q.; Sjoblom, J.; Xu, Z. Problematic Stabilizing Films in Petroleum Emulsions: Shear Rheological Response of Viscoelastic Asphaltene Films and the Effect on Drop Coalescence. *Langmuir* **2014,** *30* (23), 6730-6738.

17.   Bouriat, P.; El Kerri, N.; Graciaa, A.; Lachaise, J. Properties of a Two-Dimensional Asphaltene Network at the Water−Cyclohexane Interface Deduced from Dynamic Tensiometry. *Langmuir* **2004,** *20* (18), 7459-7464.

18.   Yarranton, H. W.; Sztukowski, D. M.; Urrutia, P. Effect of interfacial rheology on model emulsion coalescence: I. Interfacial rheology. *Journal of Colloid and Interface Science* **2007,** *310* (1), 246-252.

19.   Yarranton, H. W.; Urrutia, P.; Sztukowski, D. M. Effect of interfacial rheology on model emulsion coalescence: II. Emulsion coalescence. *Journal of Colloid and Interface Science* **2007,** *310* (1), 253-259.

20.   Alvarez, G.; Poteau, S.; Argillier, J. F.; Langevin, D.; Salager, J. L. Heavy oil-water interfacial properties and emulsion stability: Influence of dilution. *Energy and Fuels* **2009,** *23* (1), 294-299.

21.   Sztukowski, D. M.; Yarranton, H. W. Rheology of asphaltene-toluene/water interfaces. *Langmuir* **2005,** *21* (25), 11651-11658.

22.   Nenningsland, A. L.; Simon, S.; Sjöblom, J. Influence of Interfacial Rheological Properties on Stability of Asphaltene-Stabilized Emulsions. *Journal of Dispersion Science and Technology* **2014,** *35* (2), 231-243.

23.   Lucassen, J.; Van Den Tempel, M. Dynamic measurements of dilational properties of a liquid interface. *Chemical Engineering Science* **1972,** *27* (6), 1283-1291.

24.   Sjöblom, J.; Simon, S.; Xu, Z. Model molecules mimicking asphaltenes. *Advances in Colloid and Interface Science* **2015,** *218*, 1-16.

25.   Nalwaya, V.; Tantayakom, V.; Piumsomboon, P.; Fogler, S. Studies on Asphaltenes through Analysis of Polar Fractions. *Industrial & Engineering Chemistry Research* **2004,** *43* (23), 7682-7682.

26.   Marques, J. M., I.; Baudot, A.; Barré, L.; Guillaume, D.; Espinat, D.; Brunet, S. Asphaltenes Size Polydispersity Reduction by Nano- and Ultrafiltration Separation Methods

– Comparison with the Flocculation Method. *Oil & Gas Science and Technology* **2008,** *63* (1), 139-149.

27. Akbarzadeh, K., Hammami, A., Kharrat, A., Zhang, D., Allenson, S., Creek, J., Kabir, S., Jamaluddin, A., Marshall, A., Rodgers, R., Mullins, O., Solbakken, T. Asphaltenes: Problematic but rich in potential. *Oilfield Review* **2007**, 22-43.

28. Yen, T. F.; Erdman, J. G.; Pollack, S. S. Investigation of the Structure of Petroleum Asphaltenes by X-Ray Diffraction. *Analytical Chemistry* **1961,** *33* (11), 1587-1594.

29. Espinat, D. Application of Light, X-ray and Neutron diffusion Techniques to the study of colloidal systems. *Rev. Inst. Fr. Pet* **1991,** *45*, 775-820.

30. Groenzin, H.; Mullins, O. C. Asphaltene Molecular Size and Structure. *The Journal of Physical Chemistry A* **1999,** *103* (50), 11237-11245.

31. Groenzin, H.; Mullins, O. C.; Eser, S.; Mathews, J.; Yang, M.-G.; Jones, D. Molecular Size of Asphaltene Solubility Fractions. *Energy & Fuels* **2003,** *17* (2), 498-503.

32. Mullins, O. C. The Modified Yen Model. *Energy & Fuels* **2010,** *24* (4), 2179-2207.

33. Akbarzadeh, K.; Bressler, D. C.; Wang, J.; Gawrys, K. L.; Gray, M. R.; Kilpatrick, P. K.; Yarranton, H. W. Association Behavior of Pyrene Compounds as Models for Asphaltenes. *Energy & Fuels* **2005,** *19* (4), 1268-1271.

34. Rakotondradany, F.; Fenniri, H.; Rahimi, P.; Gawrys, K. L.; Kilpatrick, P. K.; Gray, M. R. Hexabenzocoronene Model Compounds for Asphaltene Fractions: Synthesis & Characterization. *Energy & Fuels* **2006,** *20* (6), 2439-2447.

35. Tan, X.; Fenniri, H.; Gray, M. R. Pyrene Derivatives of 2,2′-Bipyridine as Models for Asphaltenes: Synthesis, Characterization, and Supramolecular Organization. *Energy & Fuels* **2008,** *22* (2), 715-720.

36. Alshareef, A. H.; Scherer, A.; Tan, X.; Azyat, K.; Stryker, J. M.; Tykwinski, R. R.; Gray, M. R. Effect of Chemical Structure on the Cracking and Coking of Archipelago Model Compounds Representative of Asphaltenes. *Energy & Fuels* **2012,** *26* (3), 1828-1843.

37. Kuznicki, T.; Masliyah, J. H.; Bhattacharjee, S. Aggregation and Partitioning of Model Asphaltenes at Toluene−Water Interfaces: Molecular Dynamics Simulations. *Energy & Fuels* **2009,** *23* (10), 5027-5035.

38. Kuznicki, T.; Masliyah, J. H.; Bhattacharjee, S. Molecular Dynamics Study of Model Molecules Resembling Asphaltene-Like Structures in Aqueous Organic Solvent Systems. *Energy & Fuels* **2008,** *22* (4), 2379-2389.

39. Nordgård, E. L.; Landsem, E.; Sjöblom, J. Langmuir Films of Asphaltene Model Compounds and Their Fluorescent Properties. *Langmuir* **2008,** *24* (16), 8742-8751.

40. Nordgård, E. L.; Sjoblom, J. Model compounds for asphaltenes and C80 isoprenoid tetraacids. Part I: Synthesis and interfacial activities. *Journal of Dispersion Science and Technology* **2008,** *29* (8), 1114-1122.

41. Holman, M. W.; Liu, R.; Adams, D. M. Single-Molecule Spectroscopy of Interfacial Electron Transfer. *Journal of the American Chemical Society* **2003,** *125* (41), 12649-12654.

42. Pradilla, D.; Simon, S.; Sjöblom, J. Mixed interfaces of asphaltenes and model demulsifiers part I: adsorption and desorption of single components. *Colloids and Surfaces A: Physicochemical and Engineering Aspects* **2015,** *466*, 45-56.

43. Pradilla, D.; Simon, S.; Sjöblom, J. Mixed Interfaces of Asphaltenes and Model Demulsifiers, Part II: Study of Desorption Mechanisms at Liquid/Liquid Interfaces. *Energy & Fuels* **2015,** *29* (9), 5507-5518.

44. Ferri, J. K.; Gorevski, N.; Kotsmar, C.; Leser, M. E.; Miller, R. Desorption kinetics of surfactants at fluid interfaces by novel coaxial capillary pendant drop experiments. *Colloids and Surfaces A: Physicochemical and Engineering Aspects* **2008,** *319* (1-3), 13-20.

45.   Ferri, J. K.; Miller, R.; Makievski, A. V. Equilibrium and dynamics of PEO/PPO/PEO penetration into DPPC monolayers. *Colloids and Surfaces A: Physicochemical and Engineering Aspects* **2005,** *261* (1-3), 39-48.

46.   Vandebril, S.; Franck, A.; Fuller, G. G.; Moldenaers, P.; Vermant, J. A double wall-ring geometry for interfacial shear rheometry. *Rheologica Acta* **2010,** *49* (2), 131-144.

47.   Hermans, E.; Vermant, J. Interfacial shear rheology of DPPC under physiologically relevant conditions. *Soft Matter* **2014,** *10* (1), 175-186.

48.   Sollich, P. Rheological constitutive equation for a model of soft glassy materials. *Phys. Rev. E* **1998,** *58* (1), 738-759.

49.   Chang, C. H.; Franses, E. I. Adsorption dynamics of surfactants at the air/water interface: a critical review of mathematical models, data, and mechanisms. *Colloids and Surfaces A: Physicochemical and Engineering Aspects* **1995,** *100* (C), 1-45.

50.   Svitova, T. F.; Wetherbee, M. J.; Radke, C. J. Dynamics of surfactant sorption at the air/water interface: Continuous-flow tensiometry. *Journal of Colloid and Interface Science* **2003,** *261* (1), 170-179.

51.   Ravera, F.; Loglio, G.; Kovalchuk, V. I. Interfacial dilational rheology by oscillating bubble/drop methods. *Current Opinion in Colloid & Interface Science* **2010,** *15* (4), 217-228.

52.   Yeung, A.; Dabros, T.; Masliyah, J.; Czarnecki, J. Micropipette: a new technique in emulsion research. *Colloids and Surfaces A: Physicochemical and Engineering Aspects* **2000,** *174* (1–2), 169-181.

53.   Derkach, S. R.; Krägel, J.; Miller, R. Methods of measuring rheological properties of interfacial layers (Experimental methods of 2D rheology). *Colloid Journal* **2009,** *71* (1), 1-17.

54.   Reichert, M. D.; Alvarez, N. J.; Brooks, C. F.; Grillet, A. M.; Mondy, L. A.; Anna, S. L.; Walker, L. M. The importance of experimental design on measurement of dynamic interfacial tension and interfacial rheology in diffusion-limited surfactant systems. *Colloids and Surfaces A: Physicochemical and Engineering Aspects* **2015,** *467*, 135-142.

55.   Srivastava, S.; Leiske, D.; Basu, J. K.; Fuller, G. G. Interfacial shear rheology of highly confined glassy polymers. *Soft Matter* **2011,** *7* (5), 1994-2000.

56.   Van Hooghten, R.; Imperiali, L.; Boeckx, V.; Sharma, R.; Vermant, J. Rough nanoparticles at the oil-water interfaces: their structure, rheology and applications. *Soft Matter* **2013,** *9* (45), 10791-10798.

57.   Nordgård, E. L.; Sørland, G.; Sjöblom, J. Behavior of asphaltene model compounds at W/O interfaces. *Langmuir* **2010,** *26* (4), 2352-2360.

58.   Nenningsland, A. L.; Simon, S.; Sjöblom, J. Surface properties of basic components extracted from petroleum crude oil. *Energy and Fuels* **2010,** *24* (12), 6501-6505.

59.   Chang, H. C.; Tsen, C. H.; Chang, C. H. A model for simulating the dynamic surface tension behavior of aqueous surfactant dispersions. *Colloid and Polymer Science* **2006,** *285* (1), 57-63.

60.   Spiecker, P. M.; Gawrys, K. L.; Kilpatrick, P. K. Aggregation and solubility behavior of asphaltenes and their subfractions. *Journal of Colloid and Interface Science* **2003,** *267* (1), 178-193.

61.   Hemmingsen, P. V.; Kim, S.; Pettersen, H. E.; Rodgers, R. P.; Sjöblom, J.; Marshall, A. G. Structural Characterization and Interfacial Behavior of Acidic Compounds Extracted from a North Sea Oil. *Energy & Fuels* **2006,** *20* (5), 1980-1987.

62.   Zhang, L. Y.; Lopetinsky, R.; Xu, Z.; Masliyah, J. H. Asphaltene Monolayers at a Toluene/Water Interface. *Energy & Fuels* **2005,** *19* (4), 1330-1336.

63.   Pauchard, V.; Rane, J. P.; Banerjee, S. Asphaltene-Laden Interfaces Form Soft Glassy Layers in Contraction Experiments: A Mechanism for Coalescence Blocking. *Langmuir* **2014,** *30*, 12795-12803.

64.   Strassne, J. Effect of pH on interfacial films and stability of crude oil-water emulsions. *Journal of Petroleum Technology* **1968,** *20*, 303-312.

Figure 1. Influence of pH on the equilibrium interfacial tension values and the apparent elastic dilatational modulus of C5PeC11 at 0.05mM in toluene after 30min of equilibration. The solid lines are visual aids.
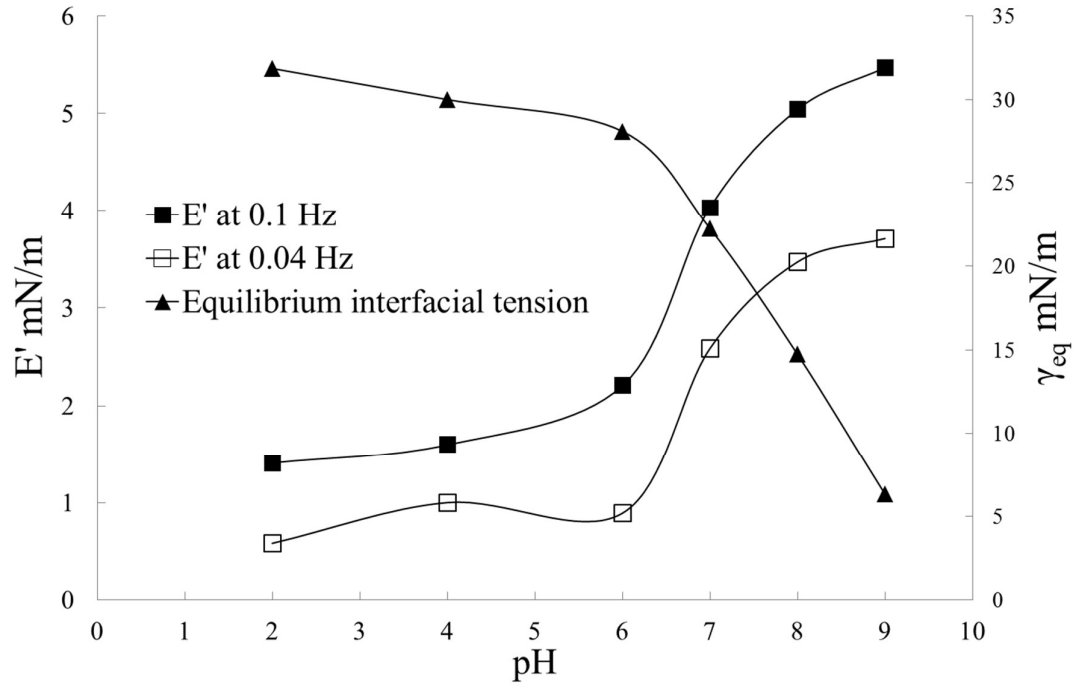
Figure 2. Equilibrium interfacial tension (γ_{eq}) as a function of the bulk concentration for C5PeC11 solutions in toluene after 30 min of equilibration time. Experimental points measured using ADSA. The solid line represents the best fit to equations (1) and (2). Equilibrium parameters are also shown.

$K_L = 709 \text{ m}^3/\text{mol}$
$\Gamma_\infty = 2.26 \times 10^{-6} \text{ mol/m}^2$
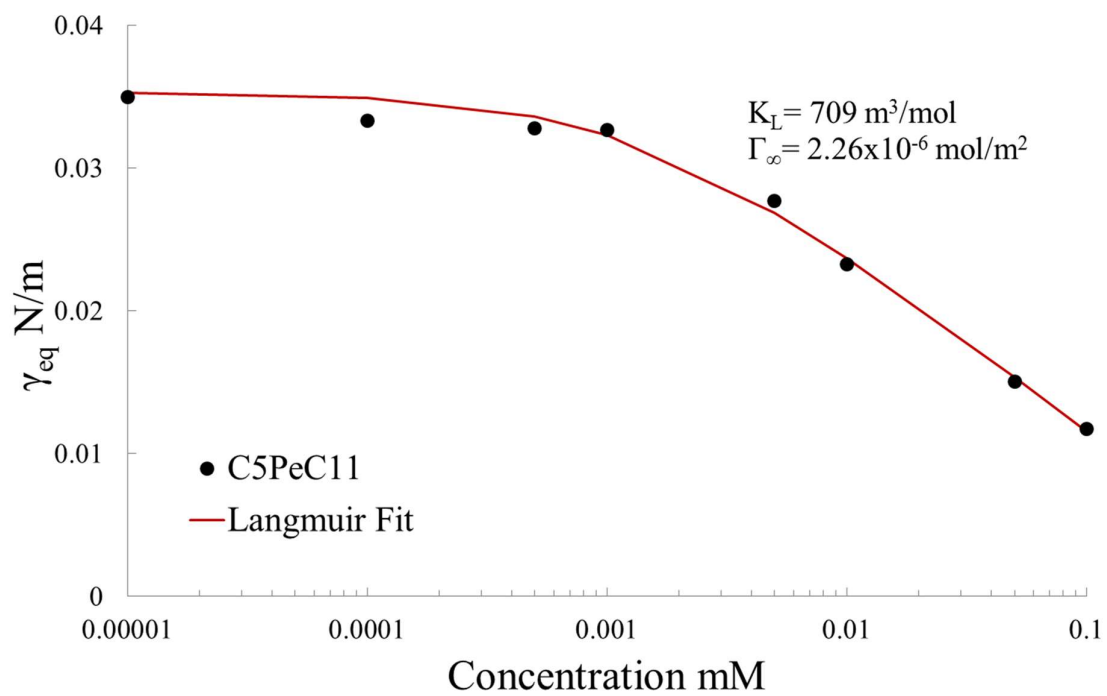
Figure 3. Measured (after 30 min of equilibration time) and modeled a) Apparent elastic modulus and b) Apparent viscous modulus of C5PeC11 solutions in toluene at different frequencies and bulk concentrations. The solid lines show the best fit with a diffusion coefficient of $4 \times 10^{-10} m^2/s$ using the Lucassen van den Tempel model (equations (6) and (7)).

a)

b)
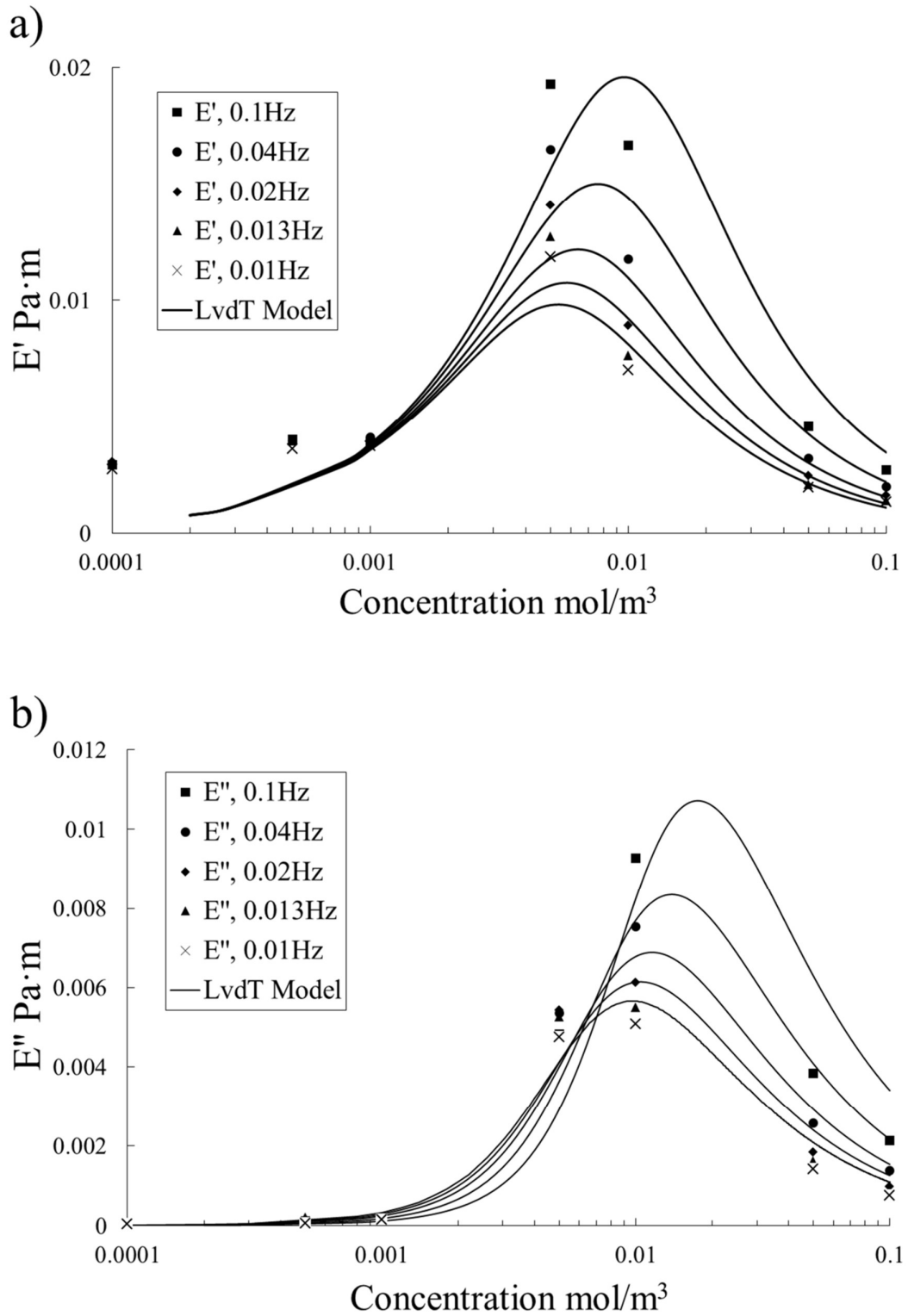
**Figure 4.** Interfacial tension as a function of the dimensionless characteristic time for desorption (Qt/V_D) of C5PeC11 at three different concentrations by toluene. The experimental conditions for the experiments were: Exchange flow rate $Q = 0.4\,\mu L/s$,total predetermined volume $V_E = 1000\,\mu L$ and volume of the droplet $V_D = 18\,\mu L$ The solid red line represents the desorption model based on equation (3).
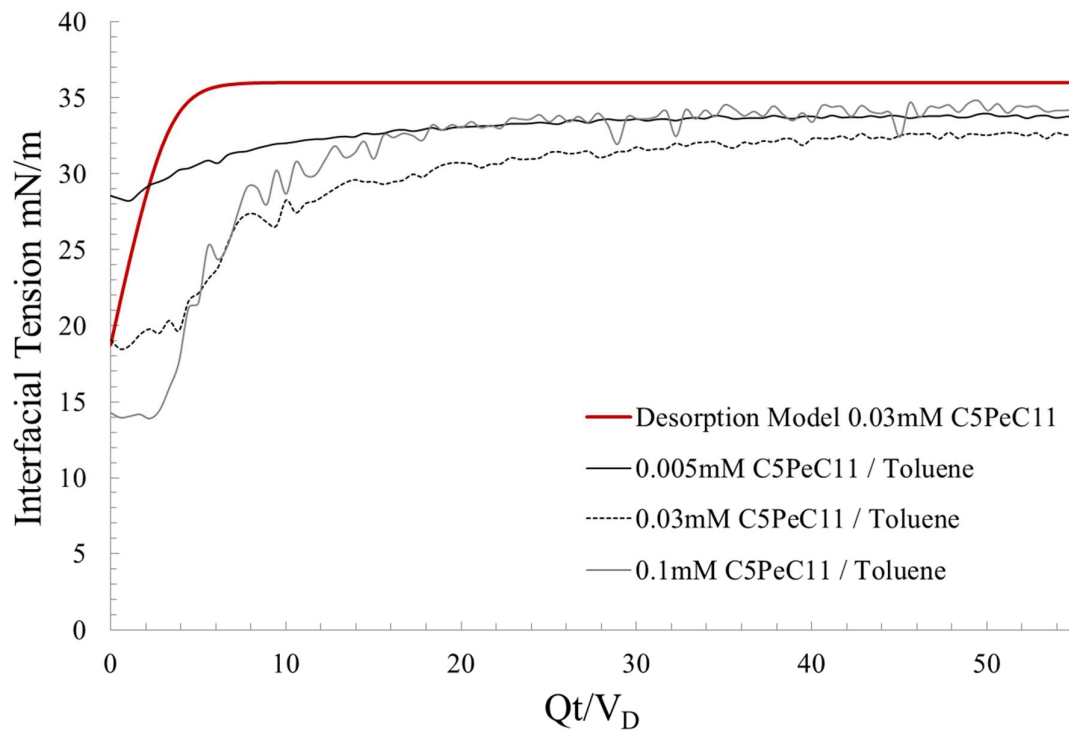
Figure 5. Interfacial tension as a function of the dimensionless characteristic time for desorption (Qt/V_D) of C5PeC11 (0.1mM in toluene) by toluene (open symbols) and BisAC11 solutions in toluene at 0.05mM (solid line) and 1.74mM (dashed line). Filled symbols represent desorption of C5PeC11 (solutions in a mixture of heptane and toluene, HepTol at 30/70 %v/v) desorbed by the same HepTol mixture. The experimental conditions for the experiments were: Exchange flow rate $Q = 0.4\ \mu L/s$, total predetermined volume $V_E = 1000\ \mu L$ and volume of the droplet $V_D = 18\ \mu L$

○ 0.1mM C5PeC11 / Toluene
▲ 0.1mM C5PeC11 / HepTol
── 0.1mM C5PeC11 / 0.05mM BisAC11
- - - 0.1mM C5PeC11 / 1.74mM BisAC11
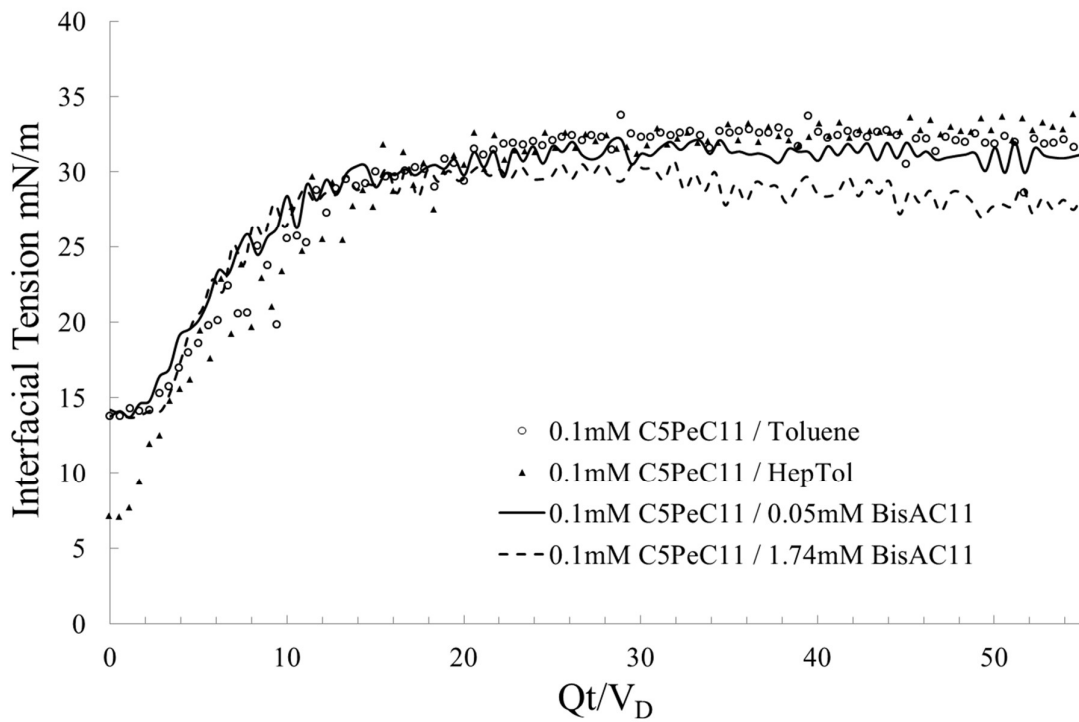
Figure 6. Compression-expansion curves for C5PeC11 at an air water interface of pH 6. Consecutive cycles of compression-expansions show (a) evidence of aggregation when large surface pressures are achieved, and (b) complete reversibility when surface pressure is kept below 30 mN/m.
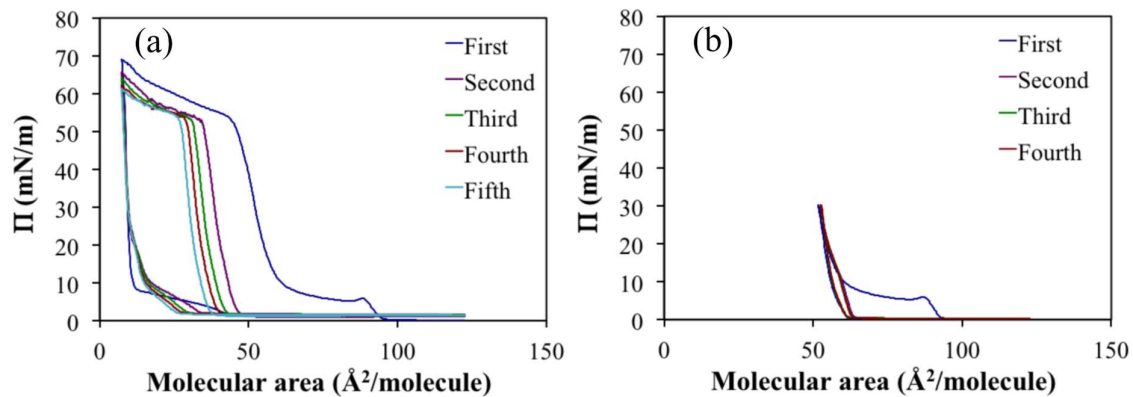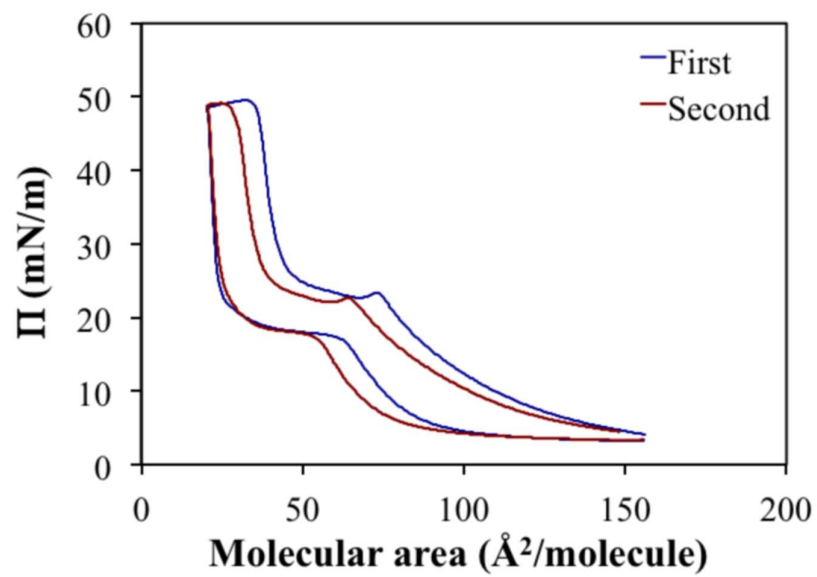
Figure 7. Dynamic moduli of C5PeC11 at an air/water interface (pH 6) at 30 mN/m as a function of (a) strain, and as a function of (b) frequency.
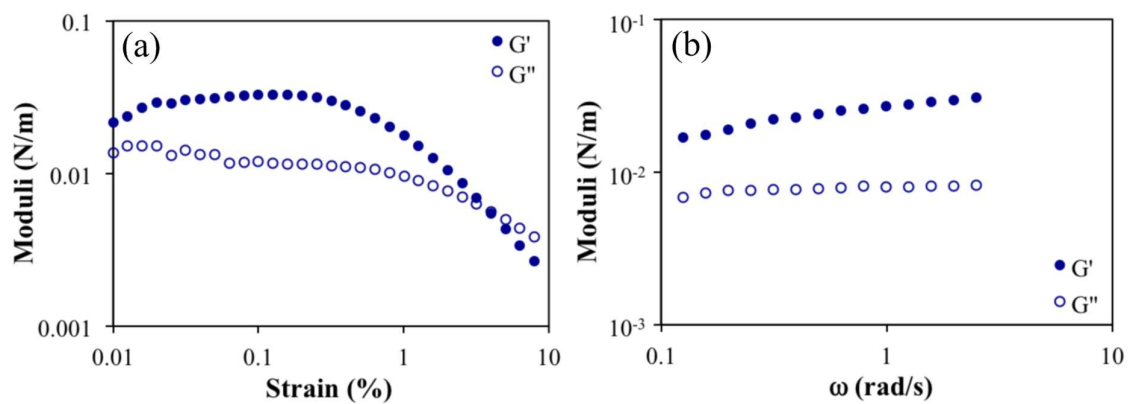
Figure 8. Compression-expansion curves from C5PeC11 at a decane/water interface. Two consecutive cycles are shown with a sub-phase pH of 6.

Figure 9. Dynamic moduli of C5PeC11 at an decane/water interface (pH 6) as a function of (a) strain, and as a function of (b) frequency. The surface pressure was 30 mN/m.
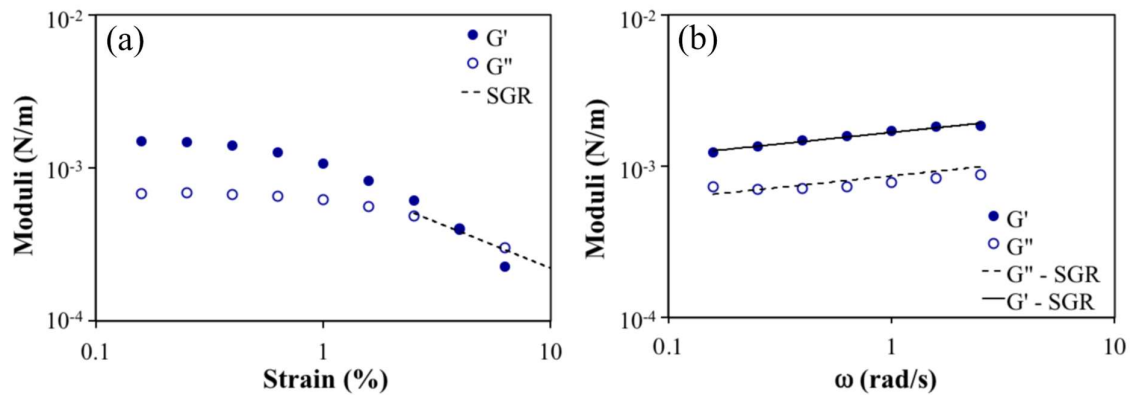
Figure 10. (a) Compression curves for C5PeC11 at a decane/water interface. The pH of the subphase was controlled with a buffer solution. Increasing pH deprotonates the carboxylate functional group of C5PeC11, increases surface activity and decreases molecular tilt at the interface. (b), (c) Conceptual drawing showing the effect of pH on molecular tilt.
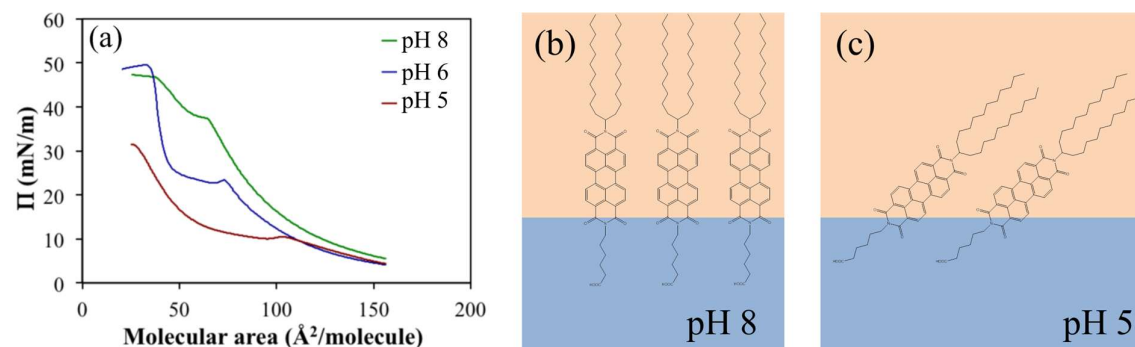
Table of contents graphic

Coupled analysis between sorption experiments (adsorption and desorption from the liquid-liquid interface) and shear/dilatational rheology experiments (at the liquid-liquid and liquid-air interface) for asphaltene model compounds.